

# Nanostructured Catalysts of Methanol Electrooxidation Based on Platinum–Ruthenium–Palladium and Platinum–Ruthenium–Iridium Alloys Derived from Coordination Compounds

N. A. Maiorova<sup>a</sup>, V. A. Grinberg<sup>a</sup>, A. A. Pasynskii<sup>b, \*</sup>, A. D. Modestov<sup>a</sup>,  
A. A. Shiryaev<sup>a</sup>, and V. V. Vysotskii<sup>a</sup>

<sup>a</sup>*Frumkin Institute of Physical Chemistry and Electrochemistry, Russian Academy of Sciences,  
Moscow, 119991 Russia*

<sup>b</sup>*Kurnakov Institute of General and Inorganic Chemistry, Russian Academy of Sciences,  
Moscow, 119991 Russia*

\*e-mail: aapasgugl@gmail.com

Received December 4, 2017

**Abstract**—Activities of the synthesized trimetallic catalysts PtRuPd/C and PtRuIr/C supported on highly dispersed carbon soot from solutions of coordination compounds of the corresponding metals are studied in the electrooxidation of methanol. According to the data of voltammetry, the Pt<sub>0.43</sub>Ru<sub>0.47</sub>Pd<sub>0.1</sub>/C and Pt<sub>0.44</sub>Ru<sub>0.46</sub>Ir<sub>0.1</sub>/C catalysts are not inferior to the commercial catalyst Pt<sub>0.5</sub>Ru<sub>0.5</sub>/C in specific characteristics, which is consistent with the data of structural studies and the electrochemical and power characteristics of the membrane electrode unit tested in the composition of a single methanol/air fuel cell.

**Keywords:** nanoelectrocatalysts, specific activity, electrooxidation

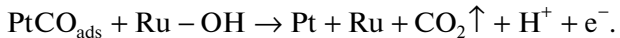
**DOI:** 10.1134/S1070328418100081

## INTRODUCTION

Fuel elements for the direct electrooxidation of alcohols demanding no reforming of the fuel used are especially attractive due to a significant simplification of their structure. The latter is one of the decisive factors for the development of an efficient power source for portable devices. Comparatively low working temperatures (25–130°C) when using solid polymer electrolytes as membranes of fuel cells are among other advantages of the fuel cells for the direct oxidation of alcohols, in particular, methanol. At the same time, a fairly low rate of methanol electrooxidation caused by the insufficient activity of the available anodic catalysts remains to be one of the yet unsolved problems. Therefore, large catalyst loads should be used to provide satisfactory exploitation characteristics (specific power and efficiency) of these fuel cells.

The oxidation of methanol on various electrode-catalysts is being studied for several decades. A detailed scheme of this process on platinum has first been proposed in [1, 2]. The authors showed that methanol oxidation proceeded via several stages, the first of which is the destructive adsorption of a methanol molecule on platinum to form a ·C–OH species, which is linked to the electrode surface by three adsorption sites and then is oxidized to CO<sub>ads</sub> with OH<sub>ads</sub> groups adsorbed on platinum and formed by the

electrochemical dissociation of water. The authors believe that it is CO as a particle most strongly bound to the metallic surface that is responsible for the overall rate of the process. The electrooxidation of methanol on the PtRu catalyst, in opinion of many researchers [2, 3], can also proceed via the bifunctional mechanisms when the chemisorption and dehydrogenation of a methanol molecule occur on the Pt atom, whereas the oxidation of the chemisorbed CO particles involves the OH groups predominantly adsorbed on ruthenium as follows:



The product of the destructive adsorption of methanol can be presented in the modern terms as a carbyne platinum complex with a strong triple bond. This coordinated carbyne species Pt≡C–OH is then attacked by the OH groups bound to platinum, CO<sub>2</sub> is evolved, and Pt–H is formed as a proton and electron source. The role of ruthenium is that this metal can be  $\pi$ -coordinated with the Pt≡C–OH triple bond, and the OH group at the ruthenium atom can also attack the carbyne bond to form CO<sub>2</sub> and a Pt–H–Ru bridge. Moreover, the carbyne moiety is capable, similarly of acetylene, of coordinating two and even three ruthenium atoms, which explains the role of the Ru : Pt ratio marked below.

The results of investigations of the catalytic activity of highly dispersed particles of the PtRu alloys for the preparation of efficient anodic catalysts for methanol oxidation were published [3–9]. Among the factors affecting the activity of the PtRu/C catalysts are the following: the alloy composition [4, 10], uniformity of the distribution, the morphology and particle size [10, 11] (depending on the preparation method), the electronic state [12–14], the presence of impurities affecting the characteristics of these catalysts, and the properties of carbon supports [15, 16]. The maximum of the catalytic activity in methanol oxidation is observed at the equiatomic ratio of platinum and ruthenium [4]. According to other data, the activity maximum is achieved at a platinum content of 20–25 at % [17].

The method for the preparation of PtRu nanoparticles on the carbon support was developed using impregnation with a mixture of platinum and ruthenium acetylacetones from the vapor phase followed by thermolysis [18]. The obtained alloy particles are characterized by a small size and are uniformly distributed over the support surface. This catalyst demonstrated high specific characteristics in the oxidation of methanol [19]. A similar procedure was used [20] for supporting nanoparticles of a PtRuIr ternary alloy. Iridium was chosen as the third component because the dissociative chemisorption of methanol occurs on it as on platinum. At the same time, similarly to ruthenium, iridium can be a source of OH groups bound to the surface and favoring the oxidation of strongly adsorbed CO molecules [21–24].

The route previously applied by us for the preparation of precursors based on the so-called heterometallic clusters can be an alternative for the method described above. In molecules of the heterometallic clusters, atoms of platinum and other metals surrounded by organic groups are in the rigid stoichiometric correspondence being linked either directly to each other or through the bridging groups. Another promising approach can be the transmetallation of electron-saturated or electron-excessive homonuclear clusters when the isoelectronic metal-containing fragments are substituted and a new heterometallic sulfide framework is formed. All organic moieties are eliminated upon the thermal decomposition of these compounds, and a mixed-metal or metal chalcogenide framework of a beforehand specified composition remains. It should be mentioned that the bimetallic PtRu nanoelectrocatalyst derived from the  $\text{Pt}_2\text{Ru}_4(\text{CO})_{18}$  cluster [25] demonstrated a high catalytic activity in methanol oxidation (five times higher than the activity of the commercial catalyst PtRu E-TEK) with a simultaneous twofold decrease in the platinum loads. Another example is presented by the bimetallic cluster precursors for the formation of the PdMoP nanoparticles described in [26] showing simultaneously that mesoporous material-supports are prefer-

ential for the formation of homogeneous nanoparticles.

In this work, we continue to develop the approach to the synthesis of the trimetallic electrocatalysts based on the initial individual Pt clusters and coordination compounds of Ru and Ir subjected to thermal destruction on the highly dispersed carbon supports at 450°C in a hydrogen atmosphere. It has previously been shown that a distinctive feature of similar catalysts is the high reproducibility of the composition and the uniform distribution over the carbon support, which provides the stability and reproducibility of the characteristics of the catalysts [27–33].

## EXPERIMENTAL

The PtRuPd catalyst was synthesized using a previously described procedure [33]. The PtRuIr catalyst was prepared by a similar procedure using the following initial compounds: ethoxydicyclopentadieneplatinum ethoxide ( $\text{C}_{10}\text{H}_{12}\text{OC}_2\text{H}_5)_2\text{Pt}_3(\text{OC}_2\text{H}_5)_4$ , the coordination ruthenium complex (ruthenium cymene dichloride  $(\text{CH}_3)_3\text{C}_7\text{H}_5\text{RuCl}_2$ ), and iridium bis(triphenylphosphine)carbonyl chloride ( $\text{PPh}_3)_2\text{Ir}(\text{CO})\text{Cl}$ . After cooling in argon of high purity, the obtained catalysts contained 32.8 wt % metals and 67.2 wt % carbon soot (Vulcan XC-72). The atomic ratio of the metals was close to 1 : 1 : 0.1.

The geometric parameters and structures of the catalysts in the initial state were studied on a scanning electron microscope with the Quanta 650 FEG field cathode (FEI, Netherlands). This instrument also allows one to conduct the energy dispersive X-ray analysis (EDX) of the studied objects due to an energy dispersive detector mounted in it.

X-ray diffraction analyses were conducted on an Empyrean diffractometer (Panalytical) using filtered  $\text{CuK}_\alpha$  radiation. The studies were carried out in the standard Bragg–Brentano reflection geometry. The samples were studied without using binders.

The average particle size and size distribution were determined by transmission electron microscopy (TEM) on a Philips EM-301 instrument at an accelerating voltage of 80 kV.

Electrochemical measurements were carried out in a standard glass three-electrode temperature-maintained cell. The working electrode was a disk glassy carbon electrode ( $S = 0.07 \text{ cm}^2$ ), which was polished and washed with a hot alkaline solution and water prior to dispersed layer supporting. The procedure of catalyst supporting on the electrode was described in detail [32, 33]. The total content of metals on the electrode was 2  $\mu\text{g}$ . A platinum grid with a surface area of  $\sim 10 \text{ cm}^2$  served as an auxiliary electrode, and  $\text{Hg}/\text{Hg}_2\text{SO}_4/0.5 \text{ M H}_2\text{SO}_4$  was the reference electrode. The working electrolyte was 0.5 M  $\text{H}_2\text{SO}_4$  (supporting solution) with an additive of 1 M  $\text{CH}_3\text{OH}$ . To

prepare electrolytes,  $\text{H}_2\text{SO}_4$  (special purity grade), doubly distilled methanol, and deionized water were used. All measurements were carried out at 50°C. The potentials are presented vs. hydrogen electrode in the same solution.

Three to five short pulses of a potential of 0.05 and 1.0 V were preliminarily applied on the working electrode with the supported catalyst (for the purification and activation of the surface), after which the voltammetric curve was recorded with a rate of 0.0005 V s<sup>-1</sup> in a range of 0.2–0.9 V in the electrolyte stirred with argon. The current transients at a working electrode potential of 0.5 V were measured to estimate the stationary currents of methanol oxidation under the conditions close to those of the operation of anodes of fuel cells.

Electrochemical measurements were conducted on an EL-02.06 automated potentiostat combined with a personal computer. The obtained experimental data were processed using standard computer programs.

A sample of the nanostructured catalyst PtRuIr(1:1:0.1)/C prepared by supporting the corresponding metallocomplex precursors on the surface of the Vulcan XC-72 carbon soot was chosen to study the activity of the synthesized catalyst in methanol oxidation in the composition of the membrane electrode unit based on this catalyst.

The membrane electrode unit was tested in the model of the methanol/air fuel cell in the Electro-Chem testing fuel cell (USA) with a working surface area of 5 cm<sup>2</sup> on the Hydrogenics G40 testing stage with the PS-DM Direct Methanol Unit Electrochem Inc. attachment. Oxygen without additional wetting and an excessive pressure was supplied with a rate of 100 mL min<sup>-1</sup> from the side of the cathode to provide minimum polarization. A 1 M aqueous solution of methanol at 50°C was pumped with a rate of 50 mL min<sup>-1</sup> from the side of the anode. The details of electrode preparation were described [26, 32]. The discharge characteristics of the methanol/air fuel cell were evaluated in the regime of cyclic voltammetry. Cyclic voltammograms were recorded in the range from the voltage of the open circuit to 0 V with a sweep rate of 5 mV s<sup>-1</sup> on an Elins P-45 potentiostat. The discharge characteristics of the membrane electrode unit were measured after the operating regime was achieved by prolonged cycling in the voltage range from the open circuit voltage to 0 V.

## RESULTS AND DISCUSSION

The typical spectrum of the nanostructured catalyst platinum–ruthenium–iridium is presented in Fig. 1 (for the corresponding figure of the platinum–iridium–palladium catalyst, see [33]). The compositions of the synthesized catalysts in the initial state (i.e., before electrochemical tests) calculated by the energy dispersive analysis data are given in Table 1.

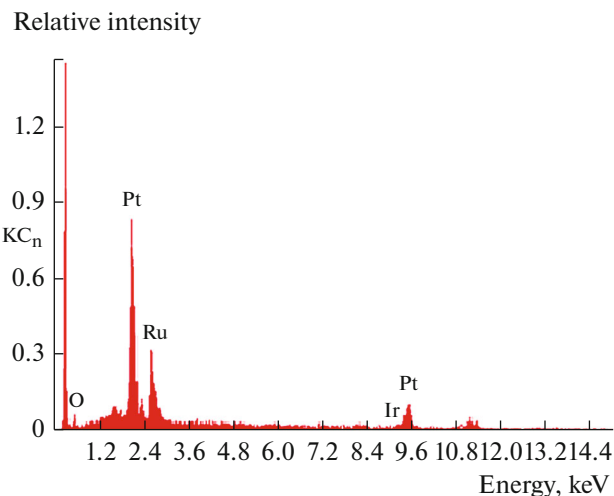


Fig. 1. Typical EDX spectrum of the PtRuIr/C catalyst.

According to the EDX data (Fig. 1), in the catalyst with Pt : Ru : Ir = 1 : 1 : 0.1, the atomic ratio of the main components in different points of the surface changes in a range of 1 : (1.0–1.28) : 0.1, which corresponds to the average composition  $\text{Pt}_{0.44}\text{Ru}_{0.46}\text{Ir}_{0.1}$ . Thus, the surface layer of the prepared PtRuIr catalyst contains both the regions where the platinum content almost corresponds to the atomic ratio specified by the synthesis and the regions with a decreased platinum content. This change in the contents of the main components in the surface layer of the catalysts can be related to the mutual diffusion of the components during preparation. A similar phenomenon of surface layer enrichment with a less noble component was observed earlier for the alloys dispersed on carbon soot [31].

The X-ray diffraction data for the PtRuIr/C, PtRuPd/C [33], and Pt/C [33] catalysts are compared in Fig. 2. A weak halo from the disordered carbon support and several broad peaks with maxima of ~40.5°, 46°, 68.6°, and 83.2° corresponding to reflections 111, 200, 220, and 311 of platinum and its solid solutions with the platinum Group elements (according to the X-ray structural data,  $c_{\text{Ir}} = 5\text{--}12\%$ ) is observed on the diffraction patterns of all samples studied. The ternary systems of the platinum Group metals are character-

Table 1. Composition of the starting catalysts

Sample	Component	wt %	at %
PtRuPd/C [33]	Pt	10.58	0.82
	Ru	6.23	0.91
	Pd	1.37	0.19
PtRuIr/C	Pt	16.57	1.42
	Ru	9.22	1.52
	Ir	3.87	0.34

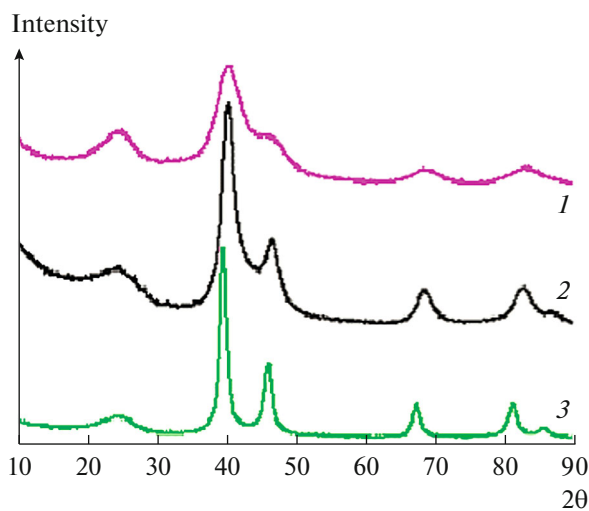


Fig. 2. Diffraction patterns of the catalyst samples: (1) PtRuIr/C, (2) PtRuPd/C [33], and (3) Pt/C [33].

ized by broad regions of the existence of solid solutions, and the composition studied lies in the single-phase region of the Pt–Ru–Ir diagram [34]. The diffraction patterns of metallic platinum and iridium themselves are fairly similar, and the presence of pure iridium isolations cannot unambiguously be denied at the observed large half-width of reflections. However, taking into account a low iridium concentration in this sample, the formation of its solid solution in platinum can be assumed with high probability, which is confirmed by the shift of peak 111 relative to pure platinum (similar shift was observed in the previously studied PtRuPd catalyst [33]).

As already mentioned, the diffraction peaks are characterized by a large half-width. The size of the coherent scattering regions for the PtRuIr/C sample

(estimated by the Scherrer equation for different crystallographic directions) is 1.5–2 nm. The phase composition of the sample was determined by comparing with the JCPDS–ICDD database and with the literature data.

The results of the PEM study of the PtRuIr catalyst are shown in Fig. 3. As can be seen from the presented TEM image and histogram of the particle size distribution, the particle size for the PtRuIr/C catalyst was 3.0–4.0 nm on the average. In addition, the sample contains an insignificant amount of particles with the size from 5 to 7 nm.

Some lack of coincidence in the particle size calculated from the X-ray diffraction and TEM data can reasonably be explained by the fact that a significant fraction of the particles is presented by twins and/or contains defects.

The voltammograms of methanol oxidation on the synthesized catalysts  $\text{Pt}_{0.43}\text{Ru}_{0.47}\text{Pd}_{0.1}/\text{C}$  and  $\text{Pt}_{0.44}\text{Ru}_{0.46}\text{Ir}_{0.1}/\text{C}$  and commercial catalyst  $\text{Pt}_{0.5}\text{Ru}_{0.5}(30\%)/\text{C}$  (Johnson Matthey) measured with a rate of  $0.5 \text{ mV s}^{-1}$  in a  $0.5 \text{ M H}_2\text{SO}_4 + 1 \text{ M CH}_3\text{OH}$  solution at  $50^\circ\text{C}$  are presented in Fig. 4. The introduction of palladium or iridium into the PtRu catalyst results in an appreciable increase in the currents detected in the potential range more positive than  $0.3 \text{ V}$  with the retention of the general character of the current dependence on the potential (Fig. 4). This indicates a higher activity of the synthesized trimetallic catalysts compared to the commercial catalyst (similar shift was also observed for the oxidation of diethyl ether on the PtRuPd catalyst [33]).

This acceleration of methanol oxidation is related, most likely, to the more efficient removal of adsorbed CO particles, which determines, as mentioned above, the overall rate of the process. The introduction of palladium or iridium into the PtRu catalyst shifts the oxi-

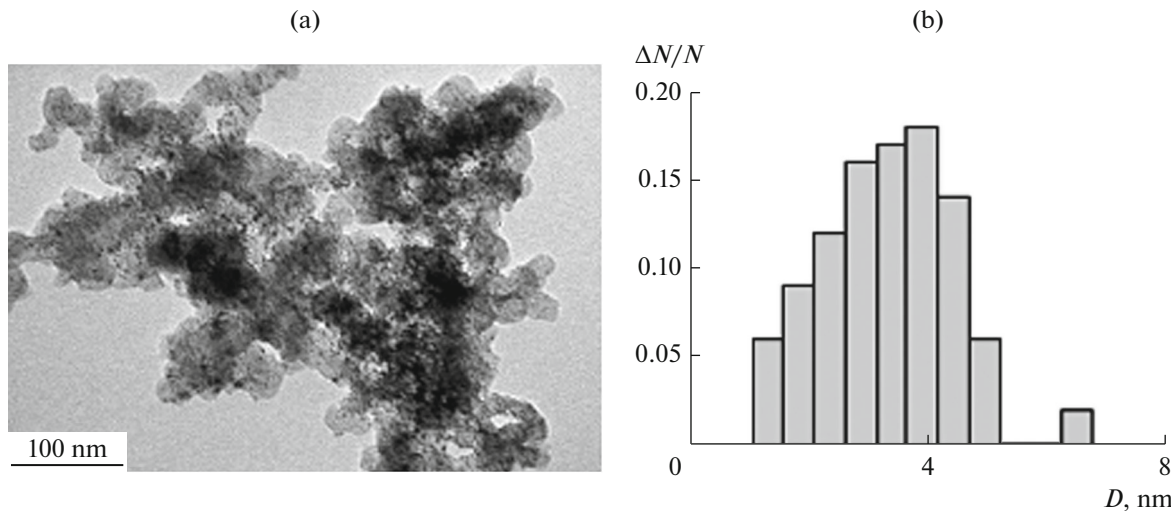
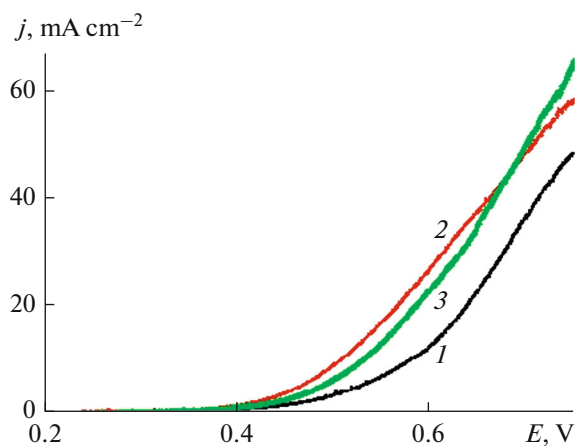


Fig. 3. (a) TEM image of the PtRuIr/C catalyst and (b) the histogram of the particle size distribution.



**Fig. 4.** Voltammograms of methanol oxidation on the (1) commercial catalyst  $\text{Pt}_{0.5}\text{Ru}_{0.5}/\text{C}$  and synthesized catalysts (2)  $\text{Pt}_{0.43}\text{Ru}_{0.47}\text{Pd}_{0.1}/\text{C}$  and (3)  $\text{Pt}_{0.44}\text{Ru}_{0.46}\text{Ir}_{0.1}/\text{C}$  measured in a  $0.5 \text{ M H}_2\text{SO}_4 + 1 \text{ M CH}_3\text{OH}$  solution at  $50^\circ\text{C}$ . The potential sweep rate is  $0.5 \text{ mV s}^{-1}$ .

dation peak of  $\text{CO}_{\text{ads}}$  to the range of lower potentials (Fig. 5), being most pronounced for the  $\text{Pt}_{0.43}\text{Ru}_{0.47}\text{Pd}_{0.1}/\text{C}$  catalyst. In addition, the surface area under the curve (amount of electricity consumed to oxidation) is increased noticeably, which is especially characteristic of  $\text{Pt}_{0.44}\text{Ru}_{0.46}\text{Ir}_{0.1}/\text{C}$ , and indicates a higher surface density of the active sites capable of binding  $\text{CO}$  and oxidizing it to  $\text{CO}_2$ . In other words, the higher activity of the synthesized trimetallic catalysts is caused by both their tolerance toward  $\text{CO}$  and a high degree of dispersity of the catalyst particles on the support surface, i.e., a larger surface area of the electrochemically active specific surface compared to that of the standard commercial catalyst. Similar results were obtained [20] for the  $\text{PtRuIr}$  catalyst prepared by the vapor phase deposition method.

The chronoamperograms of the oxidation of methanol from a 1 M solution on the trimetallic and commercial  $\text{PtRu}/\text{C}$  catalysts detected at an electrode potential of 0.5 V (electrolyte temperature  $50^\circ\text{C}$ ) are shown in Fig. 6. The time dependences of the specific currents are similar for all catalysts. The observed gradual current decrease in time is usually attributed to poisoning of the surface with intermediate products of methanol oxidation (mainly  $\text{CO}$ ) and adsorption of impurities, anions, etc. (Fig. 6). According to the voltammetry data, the synthesized catalysts  $\text{Pt}_{0.43}\text{Ru}_{0.47}\text{Pd}_{0.1}/\text{C}$  and  $\text{Pt}_{0.44}\text{Ru}_{0.46}\text{Ir}_{0.1}/\text{C}$  demonstrate substantially higher specific currents of methanol oxidation compared to those for commercial  $\text{Pt}_{0.5}\text{Ru}_{0.5}/\text{C}$ . A decrease in the activity in time is not characteristic of the  $\text{Pt}_{0.44}\text{Ru}_{0.46}\text{Ir}_{0.1}/\text{C}$  catalyst, indicating its enhanced resistance to poisoning with  $\text{CO}$  compared to other catalysts studied.

Thus, it can be concluded on the basis of the studies performed that the trimetallic catalysts

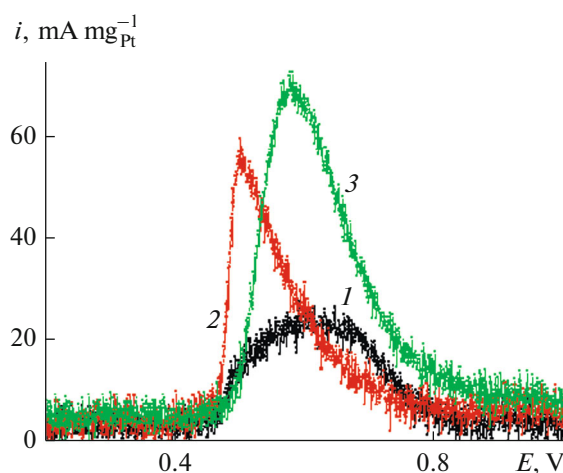


**Fig. 5.** Voltammograms of the oxidation of  $\text{CO}$  adsorbed on the synthesized catalysts (1, [33])  $\text{Pt}_{0.45}\text{Ru}_{0.55}/\text{C}$ , (2, [33])  $\text{Pt}_{0.43}\text{Ru}_{0.47}\text{Pd}_{0.1}/\text{C}$ , and (3)  $\text{Pt}_{0.44}\text{Ru}_{0.46}\text{Ir}_{0.1}/\text{C}$  measured in a potential range of  $0.2$ – $1.0 \text{ V}$  with a sweep rate of  $2 \text{ mV s}^{-1}$  in a solution of  $0.5 \text{ M H}_2\text{SO}_4$ .

$\text{Pt}_{0.43}\text{Ru}_{0.47}\text{Pd}_{0.1}/\text{C}$  and  $\text{Pt}_{0.44}\text{Ru}_{0.46}\text{Ir}_{0.1}/\text{C}$  synthesized from the coordination compounds of the corresponding metals have advantages over the bimetallic  $\text{PtRu}$  catalysts (including commercial catalysts) from the viewpoint of both their high specific activity and tolerance to  $\text{CO}$ , due to which these catalysts become very promising for the use in fuel cells for the direct oxidation of alcohols.

Since the results of testing the synthesized catalysts derived from the  $\text{PtRuPd}$  and  $\text{PtRuIr}$  alloys under model conditions showed their high electrocatalytic properties in the oxidation of methanol, one of them, namely, the  $\text{PtRuIr}/\text{C}$  catalyst, was chosen as an anodic catalyst for the preparation of the membrane electrode unit based on the commercial membrane Nafion 117, which was tested in the composition of a single methanol/air fuel cell. Commercial  $\text{Pt}(20\%)/\text{C}$  E-TEC was used as a cathodic catalyst. The results of the tests performed are illustrated in Fig. 7 presenting the dependences of the current density and power density on the voltage of the model single methanol/air fuel cell. It is established that the single methanol/air fuel cell with the synthesized anodic catalyst is not inferior to those with traditional anodic catalysts used in methanol fuel cells in current and power characteristics [35].

To conclude, the electrooxidation of methanol on the synthesized trimetallic nanoelectrocatalysts platinum–ruthenium–palladium and platinum–ruthenium–iridium supported on the highly dispersed carbon soot from solutions of the coordination compounds of the corresponding metals was studied. The synthesized catalysts  $\text{Pt}_{0.43}\text{Ru}_{0.47}\text{Pd}_{0.1}/\text{C}$  and  $\text{Pt}_{0.44}\text{Ru}_{0.46}\text{Ir}_{0.1}/\text{C}$  exceed the commercial  $\text{Pt}_{0.5}\text{Ru}_{0.5}(30\%)/\text{C}$  catalyst

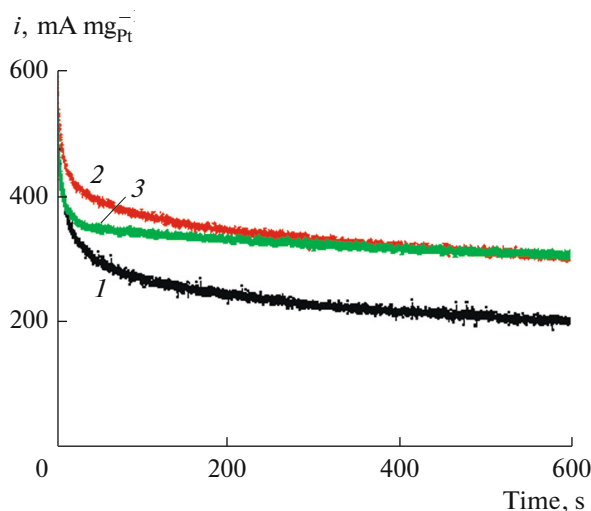


**Fig. 6.** Specific current transients of methanol oxidation at an electrode potential of 0.5 V on the (1) commercial  $\text{Pt}_{0.5}\text{Ru}_{0.5}/\text{C}$  and synthesized (2)  $\text{Pt}_{0.43}\text{Ru}_{0.47}\text{Pd}_{0.1}/\text{C}$  and (3)  $\text{Pt}_{0.44}\text{Ru}_{0.46}\text{Ir}_{0.1}/\text{C}$  catalysts measured in a 0.5 M  $\text{H}_2\text{SO}_4 + 1$  M  $\text{CH}_3\text{OH}$  solution at 50°C.

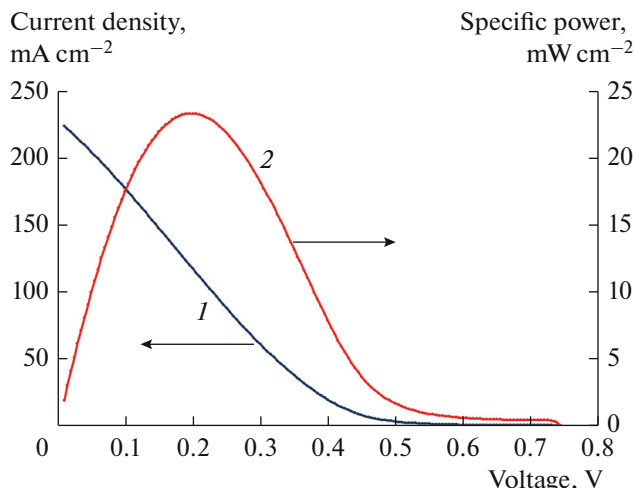


**Fig. 7.** (1) Current density and (2) power density of the discharge of the single methanol/air fuel cell with the Nafion 117 membrane, anode based on the synthesized catalyst  $\text{Pt}_{0.44}\text{Ru}_{0.46}\text{Ir}_{0.1}/\text{C}$  ( $2 \text{ mg cm}^{-2}$ ), and 20% Pt/C cathode (E-TEK,  $2.5 \text{ mg cm}^{-2}$ ); 1.0 M MeOH in water as a working solution,  $T = 50^\circ\text{C}$ .

(Johnson Matthey) in specific activity. The results of testing the membrane electrode unit with the  $\text{Pt}_{0.44}\text{Ru}_{0.46}\text{Ir}_{0.1}/\text{C}$  catalyst in the model single methanol/air fuel cell also demonstrated its high specific characteristics. Thus, the PtRuIr/C catalyst obtained from the coordination platinum clusters and coordination ruthenium and iridium compounds can be considered as a promising anodic material for using in methanol/air fuel cells.

## ACKNOWLEDGMENTS

The analytical studies were carried out on the equipment of the Center for Collective Use of the Frumkin Institute of Physical Chemistry and Electrochemistry (Russian Academy of Sciences). This work was supported by the Russian Foundation for Basic Research, project nos. 16-29-09368 and 16-03-00798.

## REFERENCES

- Vasil'ev, Yu.B. and Bagotskii, V.S., in *Uspekhi elektrokhimii organicheskikh soedinenii* (Advances in the Organic Electrochemistry), Moscow: Nauka, 1966, p. 38.
- Bagotzky, V.S. and Vassiljev, Yu.B., *Electrochim. Acta*, 1966, vol. 11, p. 1439.
- Bockris, J.O'M. and Wroblowa, H., *J. Electroanal. Chem.*, 1964, vol. 7, p. 428.
- Watanabe, M. and Motoo, M., *J. Electroanal. Chem.*, 1975, vol. 60, p. 267.
- McNicol, B.D. and Short, R.T., *J. Electroanal. Chem.*, 1977, vol. 81, p. 249.
- Goodenough, J.B., Hamnett, A., Kennedy, B.J., et al., *J. Electroanal. Chem.*, 1988, vol. 240, p. 133.
- Hamnett, A., Weeks, S.A., Kennedy, B.J., et al., *Ber. Bunsen-Ges. Phys. Chem.*, 1990, vol. 94, p. 1014.
- Jusys, Z., Kaiser, J., and Behm, R.J., *Electrochim. Acta*, 2002, vol. 47, p. 3693.
- Lu, C., Rice, C., Masel, R.I., et al., *J. Phys. Chem. B*, 2002, vol. 106, p. 9581.
- Takasu, Y., Fujiwara, T., Murakami, Y., et al., *J. Electrochem. Soc.*, 2000, vol. 147, p. 4421.
- Takasu, Y., Itaya, H., Iwazaki, T., et al., *Chem. Commun.*, 2001, p. 341.
- Hills, C.W., Nashner, M.S., Frenkel, A.I., et al., *Langmuir*, 1999, vol. 15, p. 690.
- Takasu, Y., Matsuda, Y., and Toyoshima, I., *Chem. Phys. Lett.*, 1984, vol. 108, p. 384.
- Mason, M.G., *Phys. Rev. B*, 1983, vol. 27, p. 748.
- Steigerwalt, S., Deluga, G.A., Cliffel, D.E., and Lukehart, C.M., *J. Phys. Chem. B*, 2001, vol. 105, p. 8097.
- Joo, S.H., Choi, S.J., Oh, I., et al., *Nature*, 2001, vol. 412, p. 169.
- Lizcano-Valbuena, W.H., Paganin, V.A., and Gonzalez, E.R., *Electrochim. Acta*, 2002, vol. 47, p. 3715.
- Sivakumar, P., Ishak, R., and Tricoli, V., *Electrochim. Acta*, 2005, vol. 50, p. 3312.
- Sivakumar, P. and Tricoli, V., *Electrochim. Acta*, 2006, vol. 51, p. 1235.
- Sivakumar, P. and Tricoli, V., *Electrochim. Solid-State Lett.*, 2006, vol. 9, no. 3, p. A167.
- Ortiz, R., Marquez, O.P., Marquez, J., et al., *J. Phys. Chem.*, 1996, vol. 100, p. 8389.
- Kua, J. and Goddard, W.A., *J. Am. Chem. Soc.*, 1999, vol. 121, p. 10928.
- Hamnett, A. and Kennedy, B.J., *Electrochim. Acta*, 1988, vol. 33, p. 1613.
- Liang, Y., Zhang, H., Zhong, H., et al., *J. Catal.*, 2006, vol. 238, p. 468.

25. Garcia, B.L., Captain, B., Adams, R.D., et al., *J. Clust. Sci.*, 2007, vol. 18, p. 121.
26. Grosshans-Vièles, S., Croizat, J.-L., Paillaud, P., et al., *J. Clust. Sci.*, 2008, vol. 19, p. 73.
27. Grinberg, V.A., Pasynskii, A.A., Kulova, T.L., et al., *Russ. J. Electrochem.*, 2008, vol. 44, no. 2, p. 187.
28. Grinberg, V.A., Pasynskii, A.A., Kulova, T.L., and Skundin, A.M., Abstracts of Papers, *III Ross. konf. po vodorodnoi energetike* (III Russ. Conf. on Hydrogen Power Engineering), St. Petersburg, 2006, p. 71.
29. Grinberg, V.A., Kulova, T.L., Skundin, A.M., and Pasynskii, A.A., US Patent Application 20070078052, 2007.
30. Law, C.G., Grinberg, V.A., Kulova, T.L., et al., US Patent Application 2007007011084, 2007.
31. Grinberg, V.A., Kulova, T.L., Maiorova, N.A., et al., *Russ. J. Electrochem.*, 2007, vol. 43, p. 70.
32. Maiorova, N.A., Grinberg, V.A., Emets, V.V. et al., *Russ. J. Coord. Chem.*, 2015, vol. 41, p. 817. doi 10.1134/S1070328415120052
33. Grinberg, V.A., Maiorova, N.A., Pasynskii, A.A., et al., *Russ. J. Coord. Chem.*, 2017, vol. 43, p. 206. doi 10.1134/S1070328417040017
34. Raevskaya, M.V., Vasekin, V.V., Chemleva, T.A., and Konobas, Yu.I., *Vestnik MGU, Ser. 2: Khim.*, 1984, vol. 25, no. 1, p. 109.
35. Coutancea, C., Rakotondrainibe, A.F., Lima, A., et al., *J. Appl. Electrochem.*, 2004, vol. 34, p. 61.

*Translated by E. Yablonskaya*